

# Biologically Relevant Phosphoranes: Synthesis and Structural Characterization of Glucofuranose-Derived Phosphoranes with Penta- and Hexacoordination at Phosphorus

Natalya V. Timosheva, A. Chandrasekaran, and Robert R. Holmes\*

Department of Chemistry, University of Massachusetts, Amherst, Massachusetts 01003-9336

Received August 23, 2006

Carbohydrate-based phosphoranes were synthesized by reacting the appropriate diphenol with phosphorus trichloride followed by the addition of chloralose to form **1** and by the addition of isopropylidene-D-glucofuranose to form **2** and **3**. Phosphorane **4** was obtained by reacting 1,2-*O*-isopropylidene- $\alpha$ -D-glucofuranosyl-3,5,6-phosphite (**13**) with a diphenol. For the synthesis of **5–9**, the appropriate phosphite was reacted with isopropylidene-glucofuranose. X-ray analyses of **1–9** were carried out successfully. Hexacoordinated structures resulted via oxygen donor action at phosphorus in the cases of phosphoranes **1–3** and via sulfur donor action for phosphoranes **4–6**. Trigonal bipyramidal structures formed for **7–9** with the carbohydrate components occupying axial-equatorial sites. The eight-membered ring of the diphenol moiety with weak or no donor groups in **7–9** occupied diequatorial sites of the trigonal bipyramid. Solution NMR data are in agreement with the assigned solid-state structures. Isomerism between penta- and hexacoordination is present in solution for **7**. The isomerism observed for **7** and our previous study showing a rapid exchange process that reorients the carbohydrate component of the trigonal bipyramidal phosphorane suggest that these biophosphoranes may serve as models for active sites of phosphoryl-transfer enzymes. At an active site, this type of pseudorotational behavior provides a mechanism that could bring another active site residue into play and account for a means by which some phosphoryl-transfer enzymes express promiscuous behavior.

## Introduction

Pentacoordinate phosphorus is considered an intermediate or transition state in the formation or hydrolysis of biologically relevant phosphorus compounds such as DNA, RNA, c-AMP, and several others.<sup>2</sup> In all these cases, the phosphorus is linked to the carbohydrate moiety. Phosphoranes are model compounds for the active intermediates.<sup>2</sup> Only recently have pentacoordinated monocyclic and bicyclic phosphoranes bearing the biologically relevant moieties been structurally characterized.<sup>3</sup> Only one report appears to be known that proposed a hexacoordinated ribose containing phosphorane (**A**) based on <sup>31</sup>P NMR data,<sup>4</sup> whereas two reports have

mentioned the observation of a cage containing pentacoordinate phosphoranes (**B** and **C**), but no structural information was given (Chart 1).<sup>5,6</sup> Herein, we extend our previous work<sup>3</sup> to include bicyclic and polycyclic cages containing penta- and hexacoordinated phosphoranes involving the glucofuranose derivatives **1–9** (Chart 2).

## Experimental Section

1,2-*O*-isopropylidene- $\alpha$ -D-glucofuranose (H<sub>2</sub>-gf-ip) and  $\beta$ -chloralose (H<sub>2</sub>-gf-chloral) (all Aldrich) were used as supplied. Phosphorus trichloride (Aldrich) was distilled prior to use, and triethylamine (Aldrich) was distilled over potassium hydroxide pellets. The diphenols 2,2'-sulfonylbis(6-*tert*-butyl,4-methylphenol) (**10**),<sup>7a</sup>

\* To whom correspondence should be addressed. E-mail: rrh@chem.umass.edu.

- (1) (a) Pentacoordinated Molecules part 145. (b) For part 144: Timosheva, N. V.; Chandrasekaran, A.; Holmes, R. R. *Phosphorus, Sulfur Silicon Relat. Elem.* **2006**, *181*, 1493–1511.
- (2) Holmes, R. R. *Acc. Chem. Res.* **2004**, *37*, 746–753; **1998**, *31*, 535–542, and references therein.
- (3) (a) Timosheva, N. V.; Chandrasekaran, A.; Holmes, R. R. *J. Am. Chem. Soc.* **2005**, *127*, 12474–12475. (b) Timosheva, N. V.; Chandrasekaran, A.; Holmes, R. R. *Inorg. Chem.* **2006**, *45*, 3113–3123.

- (4) Ju, Y.; Hu, J.-J.; Zhao, Y.-F. *Phosphorus, Sulfur Silicon Relat. Elem.* **2000**, *167*, 93–100.
- (5) Sychev, V. A.; Koroteev, M. P.; Dzgoeva, Z. M.; Nifant'ev, E. E. *Russ. J. Gen. Chem.* **2001**, *71*, 188.
- (6) Katalenic, D.; Skaric, V.; Klaić, B. *Tetrahedron Lett.* **1994**, *35*, 2743–2746.
- (7) (a) Chandrasekaran, A.; Day, R. O.; Holmes, R. R. *Organometallics* **1996**, *15*, 3189–3197. (b) Pastor, S. D.; Spivak, J. D.; Steinhuebel, L. P. *J. Heterocycl. Chem.* **1984**, *21*, 1285–1287.

Chart 1

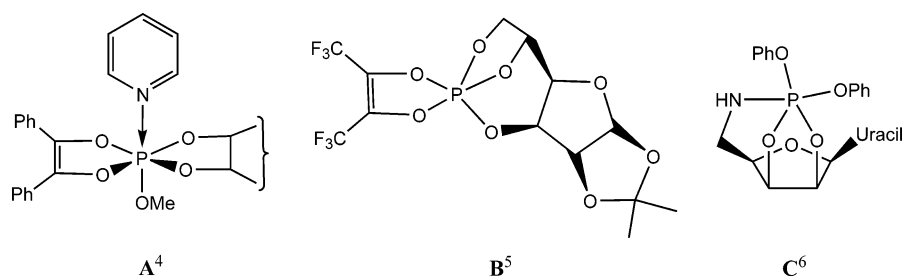
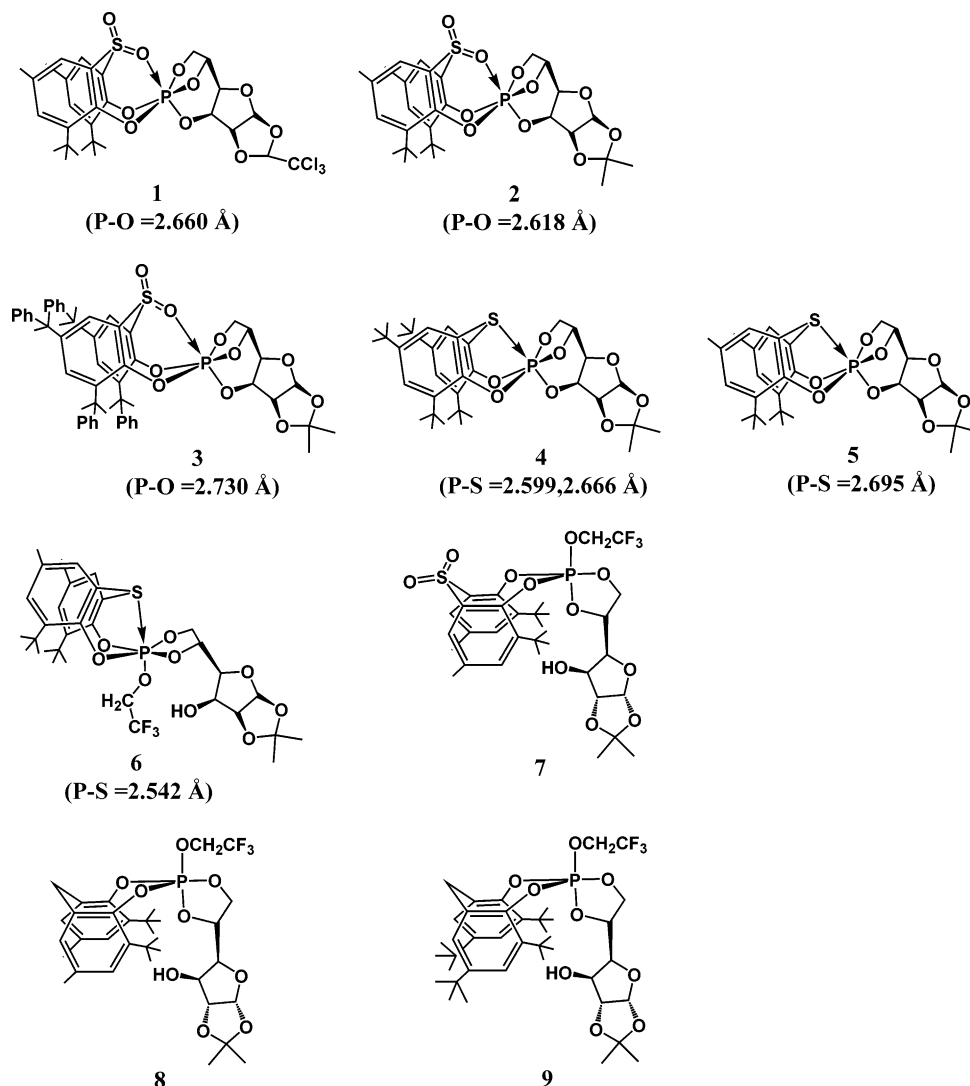


Chart 2



2,2'-sulfonylbis(bis-4,6-( $\alpha,\alpha$ -dimethylbenzyl)phenol) (**11**),<sup>1b</sup> and 2,2'-thiobis(4,6-di-*tert*-butylphenol) (**12**),<sup>7b</sup> as well as the phosphites, 1,2-*O*-isopropylidene- $\alpha$ -D-glucufuranosyl-3,5,6-phosphite (**13**),<sup>8</sup> 2,2'-thiobis(6-*tert*-butyl,4-methylphenyl)(2,2,2-trifluoroethyl)phosphite (**14**),<sup>9</sup> 2,2'-sulfonylbis(6-*tert*-butyl,4-methylphenyl)(2,2,2-trifluoroethyl)phosphite (**15**),<sup>9</sup> 2,2'-methylenebis(6-*tert*-butyl,4-methylphenyl)(2,2,2-trifluoroethyl)phosphite (**16**),<sup>9</sup> and 2,2'-methylenebis(4,6-di-*tert*-butylphenyl)(2,2,2-trifluoroethyl)phosphite (**17**),<sup>10</sup>

were synthesized according to literature methods. *N*-Chlorodiisopropylamine<sup>11</sup> was synthesized according to our earlier methods. Solvents were purified according to standard procedures.<sup>12</sup> All the reactions were carried out in an argon atmosphere. The solution NMR spectra were recorded on a Bruker Avance-400 (<sup>1</sup>H, <sup>13</sup>C), and

(8) Koroteev, M. P.; Hrebtova, S. B.; Bekker, A. R.; Pugashova, N. M.; Bel'skii, V. K.; Zotov, A. Y.; Nifant'ev, E. E. *Russ. J. Gen. Chem.* **1996**, *66*, 1576–1589.

(9) Timosheva, N. V.; Chandrasekaran, A.; Holmes, R. R. *Phosphorus, Sulfur Silicon Relat. Elem.* **2006**, *181*, 1957–1970.

(10) Abdou, W. M.; Denney, D. B.; Denney, D. Z.; Pastor, S. D. *Phosphorus, Sulfur Silicon Relat. Elem.* **1985**, *22*, 99–107.

(11) Chandrasekaran, A.; Day, R. O.; Holmes, R. R. *Inorg. Chem.* **1997**, *36*, 2578–2585.

(12) (a) Riddick, J. A.; Bunger, W. B. *Organic Solvents: Physical Properties and Methods of Purification*, 3rd ed.; Techniques of Chemistry Series; Wiley-Interscience: New York, 1970; Vol. II, Chapter V, pp 572–877. (b) Vogel, A. I. *Textbook of Practical Organic Chemistry*; Longman: London, 1978.

$^{31}\text{P}$  at 400.1, 100.6, and 162.0 MHz, respectively) spectrometer. Solution phosphorus NMR spectra were recorded in a sweep-off mode. Chemical shifts are reported in ppm, downfield positive, and relative to tetramethylsilane for  $^1\text{H}$  and  $^{13}\text{C}$  or 85%  $\text{H}_3\text{PO}_4$  for  $^{31}\text{P}$  NMR. All were recorded around 23 °C. Numberings used in  $^1\text{H}$  and  $^{13}\text{C}$  NMR data assignment are the same as those used in the X-ray analyses. The phosphorus couplings were assigned on the basis of the phosphorus decoupled proton NMR spectra. Elemental analyses were performed by the University of Massachusetts Microanalysis Laboratory.

**Syntheses.  $\text{O}_2\text{S}[\text{C}_6\text{H}_2\text{Me}(t\text{-Bu})\text{O}]_2\text{P}(\text{gf-chloral})$  (1).** A solution of diphenol **10** (4.5 g, 11.52 mmol) and phosphorus trichloride (1.0 mL, 11.43 mmol) in dichloromethane (120 mL) was stirred with *N*-chlorodiisopropylamine (1.7 mL, 11.53 mmol) for 2 h.  $\beta$ -Chloralose (3.6 g, 11.63 mmol) was added. Next, triethylamine (4.8 mL, 34.50 mmol) was added dropwise in 10 min. The reaction mixture was stirred for a further period of 48 h. The reaction mixture was washed with water (4 × 200 mL). This solution was dried over anhydrous magnesium sulfate and filtered. Solvent was removed from the filtrate. The pasty residue was recrystallized twice from hot methanol (50 mL). Yield: 0.9 g (10.8%). Single crystals containing a loosely bound dichloromethane solvate were obtained from *n*-propanol–dichloromethane (9:1) by slow evaporation. Mp: >240 °C.  $^{31}\text{P}$  NMR ( $\text{CH}_2\text{Cl}_2$ ): −54.1.  $^1\text{H}$  NMR ( $\text{CDCl}_3$ , 295 K): 1.33 (s, 9H, *t*-Bu), 1.45 (s, 9H, *t*-Bu), 2.25 (s, 3H, aryl-Me), 2.36 (s, 3H, aryl-Me), 3.79 (dd,  $^3J_{\text{POCH}} = 33.8$ , 9.1 Hz, 1H), 4.00 (dd, 9.0, 5.2 Hz, 1H), 4.13 (dt,  $^3J_{\text{POCH}} = 2.9$ , 1.9 Hz, 1H), 4.69 (ddd,  $^3J_{\text{POCH}} = 32.0$ , 5.0, 1.6 Hz, 1H), 4.92 (d, 3.0 Hz, 1H), 5.09 (d, 3.6 Hz, 1H), 5.64 (s, 1H,  $\text{CHCCl}_3$ ), 6.46 (d, 3.6 Hz, 1H, C1H), 7.32 (br, s, 1H, aryl-H), 7.36 (d, 2.0 Hz, 1H, aryl-H), 7.44 (d, 1.8 Hz, 1H, aryl-H), 7.69 (d, 1.8 Hz, 1H, aryl-H). Anal. Calcd for  $\text{C}_{30}\text{H}_{36}\text{O}_{10}\text{PSCl}_3$ : C, 49.63; H, 5.00. Found: C, 49.53; H, 4.89.

**$\text{O}_2\text{S}[\text{C}_6\text{H}_2\text{Me}(t\text{-Bu})\text{O}]_2\text{P}(\text{gf-ip})$  (2).** A solution of diphenol **10** (4.5 g, 11.52 mmol) and phosphorus trichloride (1.0 mL, 11.43 mmol) in dichloromethane (120 mL) was stirred with *N*-chlorodiisopropylamine (1.7 mL, 11.53 mmol) for 2 h. Isopropylidene-D-glucufuranose (2.5 g, 11.35 mmol) and triethylamine (4.8 mL, 34.50 mmol) were added. The reaction mixture was stirred for a further period of 24 h. The reaction mixture was washed with water (4 × 200 mL) and a saturated sodium chloride solution (100 mL). This resulting solution was dried over anhydrous magnesium sulfate and filtered. Solvent was removed from the filtrate, and the pasty residue was allowed to solidify for 2 days. The solid was stirred with ethanol (100%, 50 mL), washed with ethanol (100%, 50 mL), and air-dried. Yield: 1.2 g (16.6%). Single crystals were obtained from ethanol–dichloromethane (30–15 mL) by slow evaporation. Mp: > 200 °C (dec).  $^{31}\text{P}$  NMR ( $\text{CH}_2\text{Cl}_2$ ): −53.4.  $^1\text{H}$  NMR ( $\text{CDCl}_3$ , 295 K): 1.31 (s, 9H, *t*-Bu), 1.40 (s, 3H,  $\text{CMe}_2$ ), 1.47 (s, 9H, *t*-Bu), 1.53 (s, 3H,  $\text{CMe}_2$ ), 2.25 (s, 3H, aryl-Me), 2.36 (s, 3H, aryl-Me), 3.78 (dd,  $^3J_{\text{POCH}} = 33.3$ , 8.8 Hz, 1H), 3.97 (dd, 8.8, 5.2 Hz, 1H), 4.15 (dt,  $^3J_{\text{POCH}} = 3.0$ , 2.1 Hz, 1H), 4.66 (dd,  $^3J_{\text{POCH}} = 32.0$ , 4.3 Hz, 1H), 4.73 (d, 3.4 Hz, 1H), 4.83 (d, 2.9 Hz, 1H), 6.17 (d, 3.4 Hz, 1H, C1H), 7.31 (s, 1H, aryl-H), 7.35 (s, 1H, aryl-H), 7.43 (s, 1H, aryl-H), 7.70 (s, 1H, aryl-H). Anal. Calcd for  $\text{C}_{31}\text{H}_{41}\text{O}_{10}\text{PS}$ : C, 58.48; H, 6.49. Found: C, 58.49; H, 6.48.

**$\text{O}_2\text{S}[\text{C}_6\text{H}_2(\text{CMe}_2\text{Ph})\text{O}]_2\text{P}(\text{gf-ip})$  (3).** A mixture of diphenol **11** (4.2 g, 5.82 mmol) and phosphorus trichloride (0.5 mL, 5.73 mmol) was dissolved in dichloromethane (100 mL). To this solution was added triethylamine (1.6 mL, 11.50 mmol) in dichloromethane (50 mL) with stirring over a period of 25 min. The solution was stirred for 2 h. Isopropylidene-D-glucufuranose (1.3 g, 5.90 mmol) and *N*-chlorodiisopropylamine (0.9 mL, 6.11 mmol) were added, and the solution was stirred for a further period of 1 h. Triethylamine

(0.8 mL, 5.75 mmol) was added, and the reaction mixture was stirred for 24 h. The reaction mixture was washed with water (4 × 200 mL). The resulting solution was dried over anhydrous magnesium sulfate and filtered. Solvent was removed from the filtrate, and the pasty residue was dissolved in dichloromethane–heptane (50–25 mL). When the solution was reduced to about 50 mL, an oil formed, which was separated off. The remaining solution was stirred with anhydrous potassium bicarbonate and filtered, and the solvent was removed. The residue was extracted with toluene (20 mL), and hexane (80 mL) was added. The precipitate was extracted with ether–heptane (30–20 mL) and left for slow evaporation to obtain the pure compound as an amorphous solid. Yield: 0.7 g (12.5%). Single crystals were obtained from a chlorobenzene solution by layering with hexane solvent. Mp: 229–230 °C.  $^{31}\text{P}$  NMR ( $\text{CH}_2\text{Cl}_2$ ): −52.4.  $^1\text{H}$  NMR ( $\text{CDCl}_3$ , 295 K): 1.37 (s, 3H,  $\text{CH}_3$ ), 1.45 (s, 3H,  $\text{CH}_3$ ), 1.48 (s, 3H,  $\text{CH}_3$ ), 1.53 (s, 3H,  $\text{CH}_3$ ), 1.59 (s, 3H,  $\text{CH}_3$ ), 1.60 (s, 3H,  $\text{CH}_3$ ), 1.61 (s, 3H,  $\text{CH}_3$ ), 1.66 (s, 3H,  $\text{CH}_3$ ), 1.69 (s, 3H,  $\text{CH}_3$ ), 1.71 (s, 3H,  $\text{CH}_3$ ), 3.375 (d, 3.0 Hz, 1H), 3.383 (dd,  $^3J_{\text{POCH}} = 33.2$ , 8.8 Hz, 1H), 3.66 (dt,  $^3J_{\text{POCH}} = 3.0$ , 1.2 Hz, 1H), 3.75 (dd, 8.8, 5.1 Hz, 1H), 4.16 (d, 3.5 Hz, 1H), 4.38 (ddd,  $^3J_{\text{POCH}} = 31.7$ , 5.1, 1.2 Hz, 1H), 5.92 (d, 3.5 Hz, C1H), 6.9–7.3 (multiplets, 22H), 7.64 (d, 2.4 Hz, 1H, aryl-H), 7.92 (d, 2.4 Hz, 1H, aryl-H). Anal. Calcd for  $\text{C}_{57}\text{H}_{61}\text{O}_{10}\text{PS}$ : C, 70.64; H, 6.34. Found: C, 70.59; H, 6.43.

**$[\text{C}_6\text{H}_2(t\text{-Bu})_2\text{O}]_2\text{P}(\text{gf-ip})$  (4).** Phosphite **13** (1.0 g, 4.03 mmol) and excess diphenol **12** (5.35 g, 12.08 mmol) were stirred in dichloromethane (40 mL). *N*-Chlorodiisopropylamine (1.8 mL, 12.20 mmol) was added, and the solution was stirred for 1 week. The reaction mixture was washed with water (4 × 100 mL), and the volume was adjusted to 50 mL with dichloromethane. An equal volume of heptane was added. The solution was dried over anhydrous magnesium sulfate and filtered. The solution was then subjected to fractional crystallization from heptane (20 mL final volume), acetonitrile (50 mL), hexane (40 mL), and methanol (15 mL to a final volume of 7 mL); at each stage, any solid product was successively discarded. The final methanol solution was cooled to remove additional orange solid. Then the solution was allowed to evaporate, and the oil was left for 1 week to solidify. This solid was washed with hexane (4 × 5 mL) to yield a colorless powder. Yield: 0.125 g (4.5%). Mp: 220 °C (dec). Single crystals suitable for X-ray studies were obtained from heptane–dichloromethane (2–1 mL) by slow evaporation.  $^{31}\text{P}$  NMR ( $\text{CH}_2\text{Cl}_2$ ): −59.6.  $^1\text{H}$  NMR ( $\text{CDCl}_3$ , 295 K): 1.26 (s, 18H, *t*-Bu), 1.36 (s, 9H, *t*-Bu), 1.37 (s, 9H, *t*-Bu), 1.39 (s, 3H,  $\text{CMe}_2$ ), 1.52 (s, 3H,  $\text{CMe}_2$ ), 3.89 (dd,  $^3J_{\text{POCH}} = 22.4$ , 9.2 Hz, 1H), 3.94 (br, 1H), 4.07 (q, br, 2.0 Hz, 1H), 4.50 (dd,  $^3J_{\text{POCH}} = 33.4$ , 4.0 Hz, 1H), 4.78 (d, 2.6 Hz, 1H), 4.81 (d, 3.4 Hz, 1H), 6.05 (d, 3.4 Hz, 1H, C1H), 7.31 (s, 2H, aryl-H), 7.42 (d, 2.2 Hz, 1H, aryl-H), 7.43 (d, 2.2 Hz, 1H, aryl-H). Anal. Calcd for  $\text{C}_{37}\text{H}_{53}\text{O}_8\text{PS}$ : C, 64.51; H, 7.75. Found: C, 64.48; H, 7.67.

**$[\text{C}_6\text{H}_2\text{Me}(t\text{-Bu})\text{O}]_2\text{P}(\text{gf-ip})$  (5) and  $[\text{C}_6\text{H}_2\text{Me}(t\text{-Bu})\text{O}]_2\text{P}(\text{OCH}_2\text{CF}_3)(\text{gf-ip})$  (6).** Phosphite **14** (3.10 g, 6.37 mmol) and isopropylidene-D-glucufuranose (1.40 g, 6.36 mmol) were stirred in dichloromethane (110 mL). *N*-Chlorodiisopropylamine (1.0 mL, 6.78 mmol) was added, and the solution was stirred for 21 h. Solvent was removed from the reaction mixture, and the residue was extracted with ether (120 mL) and filtered off. Heptane (20 mL) was added, and the solution was left under an argon flow. When the solution was reduced to about 60 mL, the solution was filtered to remove some precipitate. The filtrate was left under an argon flow again. When the solvent volume was reduced to about 20 mL, the solution was decanted and the solid was washed with heptane (10 mL) and air-dried. The  $^{31}\text{P}$  NMR of the colorless solid showed

the presence of three phosphoranes ( $-47.2$ ,  $-48.5$ , and  $-55.7$  ppm in toluene). Recrystallization of this colorless solid from hexane–dichloromethane (1:1) provided a few crystals of **5** and **6**. Repeated attempts at further crystallization did not provide any pure isomer. The decanted solution gave a yellow oil that solidified to a yellow powder. The powder was dissolved in ethanol (90 mL), precipitated with water (12 mL), and air-dried. This removed the phosphate impurity. The  $^{31}\text{P}$  NMR spectrum of the yellow powder showed the presence of several (about 20) phosphoranes in three distinct regions ( $-48$  to  $-53$ ,  $-73$  to  $-77$ , and  $-85$  to  $-89$  ppm). This yellow powder was soluble in all common organic solvents (from hexane to ethanol), and hence no crystalline product or any pure isomer could be obtained. Yield: colorless solid (1.0 g) and yellow powder (0.8 g) (40%). Mp for crystals of **6**:  $157$ – $160$  °C. Anal. Calcd for  $\text{C}_{33}\text{H}_{44}\text{O}_9\text{F}_3\text{P}$ : C, 56.24; H, 6.29. Found (colorless solid): C, 56.32; H, 6.53.  $^{31}\text{P}$  NMR for **5** ( $\text{CD}_2\text{Cl}_2$ ):  $-57.2$ .  $^1\text{H}$  NMR ( $\text{CDCl}_3$ , 295 K) for **5**: 1.33 (s, 9H, *t*-Bu), 1.35 (s, 9H, *t*-Bu), 1.38 (s, 3H,  $\text{CMe}_2$ ), 1.52 (s, 3H,  $\text{CMe}_2$ ), 2.22 (s, 3H, aryl- $\text{CH}_3$ ), 2.23 (s, 3H, aryl- $\text{CH}_3$ ), 3.87 (dd,  $^3J_{\text{POCH}} = 37.3$ , 9.1 Hz, 1H), 3.91 (d, 2.6 Hz, 1H), 4.07 (q, 2.5 Hz, 1H), 4.55 (m, 1H), 4.76 (d, 2.8 Hz, 1H), 4.78 (d, 3.6 Hz, 1H), 6.06 (d, 3.5 Hz, 1H, C1H), 7.05 (s, br, 2H, aryl-H), 7.22 (d, 1.8 Hz, 1H, aryl-H), 7.24 (d, 1.8 Hz, 1H, aryl-H).  $^{31}\text{P}$  NMR for **6** ( $\text{CH}_2\text{Cl}_2$ ):  $-58.5$ . Proton NMR for **6** could not be obtained due to the decomposition of the pure crystals. The crystals of **5** were not pure enough to get analyses or a melting point.

$\text{O}_2\text{S}[\text{C}_6\text{H}_2\text{Me}(t\text{-Bu})\text{O}]_2\text{P}(\text{OCH}_2\text{CF}_3)(\text{gf-ip})$  (**7**). Phosphite **15** (1.3 g, 2.51 mmol) and isopropylidene-glucosylfuranose (0.55 g, 2.50 mmol) were stirred in dichloromethane (100 mL). *N*-Chlorodiisopropylamine (0.4 mL, 2.71 mmol) was added, and the solution was stirred for 24 h. Solvent was removed from the reaction mixture, and the residue was extracted with ether (120 mL) and filtered off. Solvent was removed from the filtrate, and the residue was redissolved in dichloromethane–heptane (20:20 mL). The solution was left under an argon flow to obtain a crystalline solid. Yield: 0.40 g (22%). Mp:  $224$ – $227$  °C (dec).  $^{31}\text{P}$  NMR ( $\text{CH}_2\text{Cl}_2$ ):  $-60.4$ ,  $-49.6$  (integral ratio 2.7:1).  $^1\text{H}$  NMR ( $\text{CDCl}_3$ , 295 K):  $-0.88$  (d, 2.6 Hz, 1H, OH), 1.18 (s, 3H,  $\text{CMe}_2$ ), 1.31 (s, 3H,  $\text{CMe}_2$ ), 1.43 (s, 9H, *t*-Bu), 1.45 (s, 9H, *t*-Bu), 2.39 (s, 6H, aryl- $\text{CH}_3$ ), 2.51 (s, 1H), 3.04 (dd, 9.0, 2.4 Hz, 1H), 3.19 (q, 8.5 Hz, 1H), 3.68 (td, 9.2, 6.4 Hz), 4.02 (dd, 9.1, 7.4 Hz, 1H), 4.08 (d, 3.5 Hz, 1H), 4.68 (m,  $\text{OCH}_2\text{CF}_3$ , 2H), 5.60 (d, 3.6 Hz, 1H, C1H), 7.39 (s, 1H, aryl-H), 7.44 (s, 1H, aryl-H), 7.77 (d, 1.8 Hz, 1H, aryl-H), 7.80 (d, 1.8 Hz, 1H, aryl-H). Anal. Calcd for  $\text{C}_{33}\text{H}_{44}\text{O}_{11}\text{F}_3\text{P}$ : C, 53.80; H, 6.02. Found: C, 53.76; H, 6.09.

$\text{CH}_2[\text{C}_6\text{H}_2\text{Me}(t\text{-Bu})\text{O}]_2\text{P}(\text{OCH}_2\text{CF}_3)(\text{gf-ip})$  (**8**). Phosphite **16** (1.60 g, 3.42 mmol) and isopropylidene-glucosylfuranose (0.75 g, 3.41 mmol) were stirred in dichloromethane (60 mL). *N*-Chlorodiisopropylamine (0.5 mL, 3.39 mmol) was added, and the solution was stirred for 24 h. Solvent was removed from the reaction mixture, and the residue was extracted with ether (100 mL) and filtered off. Heptane (40 mL) was added, and the solution was left under an argon flow. The crystalline solid that formed was separated by decanting the mother liquor and washing the solid with hexane. Yield: 1.0 g (43%). Mp:  $168$ – $171$  °C (dec).  $^{31}\text{P}$  NMR ( $\text{CH}_2\text{Cl}_2$ ):  $-54.5$ .  $^1\text{H}$  NMR ( $\text{CDCl}_3$ , 295 K):  $-0.08$  (d, 3.5 Hz, 1H, OH), 1.17 (s, 3H,  $\text{CMe}_2$ ), 1.31 (s, 3H,  $\text{CMe}_2$ ), 1.38 (s, 9H, *t*-Bu), 1.41 (s, 9H, *t*-Bu), 2.33 (s, 3H, aryl- $\text{CH}_3$ ), 2.34 (s, 3H, aryl- $\text{CH}_3$ ), 2.45 (s, 1H), 3.21 (m, 2H), 3.49 (d, 13.7 Hz, 1H,  $\text{CH}_2$ ), 3.65 (q, 6.5 Hz, 1H), 4.06 (m, 2H), 4.23 (dd, 13.6, 2.7 Hz, 1H,  $\text{CH}_2$ ), 4.52 (dq, 8.6, 4.4 Hz, 2H,  $\text{OCH}_2\text{CF}_3$ ), 5.62 (d, 3.4 Hz, C1H), 7.00 (s, 1H, aryl-H),

7.07 (s, 1H, aryl-H), 7.14 (s, 1H, aryl-H), 7.15 (s, 1H, aryl-H). Anal. Calcd for  $\text{C}_{34}\text{H}_{46}\text{O}_9\text{F}_3\text{P}$ : C, 59.46; H, 6.75. Found: C, 59.68; H, 6.83.

$\text{CH}_2[\text{C}_6\text{H}_2(t\text{-Bu})_2\text{O}]_2\text{P}(\text{OCH}_2\text{CF}_3)(\text{gf-ip})$  (**9**). Phosphite **17** (6.30 g, 11.4 mmol) and isopropylidene-glucosylfuranose (2.5 g, 11.4 mmol) were stirred in dichloromethane (120 mL). *N*-Chlorodiisopropylamine (1.7 mL, 11.5 mmol) was added, and the solution was stirred for 24 h. Solvent was removed from the reaction mixture, and the residue was extracted with ether (100 mL) and filtered off. The filtrate was left under an argon flow, and the solid that formed was washed with hexane ( $2 \times 30$  mL) and air-dried. Yield: 8.0 g (91%). Single crystals suitable for X-ray studies were obtained from heptane–dichloromethane (1:1) by slow evaporation. Mp:  $207$ – $209$  °C.  $^{31}\text{P}$  NMR ( $\text{CH}_2\text{Cl}_2$ ):  $-54.4$ .  $^1\text{H}$  NMR ( $\text{CDCl}_3$ , 295 K): 1.14 (s, 3H,  $\text{CMe}_2$ ), 1.30 (s, 3H,  $\text{CMe}_2$ ), 1.31 (s, 9H, *t*-Bu), 1.34 (s, 9H, *t*-Bu), 1.40 (s, 9H, *t*-Bu), 1.42 (s, 9H, *t*-Bu), 1.55 (s, 1H, OH), 2.45 (t, 2.9 Hz, 1H), 3.15 (dd, 8.8, 2.0 Hz, 1H), 3.23 (q, 8.3 Hz, 1H), 3.56 (d, 13.7 Hz, 1H,  $\text{CH}_2$ ), 3.67 (td, 9.0, 6.3 Hz, 1H), 4.00 (d, 3.5 Hz, 1H), 4.03 (ddd, 25.6, 8.8, 1.5 Hz, 1H), 4.30 (dd, 13.7, 2.6 Hz, 1H,  $\text{CH}_2$ ), 4.53 (m, 2H,  $\text{OCH}_2\text{CF}_3$ ), 5.59 (d, 3.6 Hz, C1H), 7.22 (t, 1.9 Hz, 1H, aryl-H), 7.25 (t, 1.9 Hz, 1H, aryl-H), 7.36 (t, 2.0 Hz, 2H, aryl-H). Anal. Calcd for  $\text{C}_{40}\text{H}_{58}\text{O}_9\text{F}_3\text{P}$ : C, 62.33; H, 7.58. Found: C, 62.62; H, 7.69.

**X-ray Studies.** The X-ray crystallographic studies on **1**–**9** were performed using a Nonius Kappa charge-coupled device (CCD) diffractometer and graphite-monochromated Mo  $\text{K}\alpha$  radiation ( $\lambda = 0.71073$  Å). Data were collected at 293 K,  $\theta_{\text{MoK}\alpha} \leq 25^\circ$ , but in the case of **5**,  $\theta_{\text{MoK}\alpha}$  was  $\leq 20^\circ$ . All of the data were included in the refinement. The structures were solved by direct methods and difference Fourier techniques and were refined by full-matrix least-squares analysis. Refinements were based on  $F^2$ , and computations were performed on a 2.6 GHz Pentium 4 computer using SHELXS-86 for solution<sup>13</sup> and SHELXL-97 for refinement.<sup>14</sup> All of the non-hydrogen atoms were refined anisotropically. All hydrogen atoms were included in the refinement as isotropic scatterers riding in either ideal positions or with torsional refinement (in the case of methyl hydrogen atoms) on the bonded atoms. The hydrogens on disordered atoms, on the atoms connected to the disordered atoms, and on the OH groups of **7** and **8** were not included in the calculations. The hydroxyl hydrogen in **6** was located from a difference Fourier and refined, whereas the hydroxyl hydrogen of **9** was fixed at a calculated position. The final agreement factors are based on the reflections with  $I \geq 2\sigma$ .

There were two independent molecules in the crystal lattices of **4**, **7**, and **8**. One *tert*-butyl group in **2** and **9** was disordered, and they were refined in two positions with an occupancy ratio of 70:30 and 60:40, respectively. Two of the *tert*-butyl groups in one molecule of **4** were disordered, and they were refined in two positions with a 50:50 occupancy ratio at the isotropic level. There was a poorly behaved dichloromethane molecule in the crystal lattice of **1** with the chlorines disordered across four positions with equal occupancy. Ten atoms from two bis( $\alpha,\alpha$ -dimethylbenzyl) groups in the molecule of **3** had extremely high anisotropic displacement parameters, and they were restrained. A data recollection carried out with a much smaller crystal did not improve this situation. The crystal quality of **5** was very poor because of its small size and high mosaicity. The high *R*-factor for **5**, low calculated density, and the presence of solvent accessible voids in packing analyses suggested the possible presence of solvent, but the observed residual electron densities of less than  $0.52 e/\text{\AA}^3$  and

(13) Sheldrick, G. M. *Acta Crystallogr.* **1990**, *A46*, 467.

(14) Sheldrick, G. M. SHELXL-97: Program for Crystal Structure Determination. University of Göttingen, Germany, 1997.



**Table 1.** Crystallographic Data for Compounds **1–9**

	<b>1</b>	<b>2</b>	<b>3</b>
formula	C <sub>30</sub> H <sub>36</sub> Cl <sub>3</sub> O <sub>10</sub> PS·CH <sub>2</sub> Cl <sub>2</sub>	C <sub>31</sub> H <sub>41</sub> O <sub>10</sub> PS	C <sub>37</sub> H <sub>61</sub> O <sub>10</sub> PS
fw	810.89	636.67	969.09
crystal system	orthorhombic	orthorhombic	monoclinic
space group	<i>P</i> 2 <sub>1</sub> 2 <sub>1</sub> 2 <sub>1</sub>	<i>P</i> 2 <sub>1</sub> 2 <sub>1</sub> 2 <sub>1</sub>	<i>P</i> 2 <sub>1</sub>
crystal size (mm)	1.00 × 1.00 × 0.50	0.75 × 0.10 × 0.10	1.00 × 0.40 × 0.10
<i>a</i> (Å)	11.0843(2)	9.8098(1)	11.0705(1)
<i>b</i> (Å)	12.0184(4)	14.9672(2)	12.6674(1)
<i>c</i> (Å)	28.440(1)	22.2989(4)	18.8035(3)
$\beta$ (deg)	90.00	90.00	101.4150(6)
<i>V</i> (Å <sup>3</sup> )	3788.7(2)	3274.04(8)	2584.74(5)
<i>Z</i>	4	4	2
<i>D</i> <sub>calc</sub> (g/cm <sup>3</sup> )	1.422	1.292	1.245
$\mu_{\text{MoK}\alpha}$ (cm <sup>-1</sup> )	5.32	2.01	1.52
total reflns	6495	5718	8667
reflns with <i>I</i> > 2 $\sigma$ <i>I</i>	5536	4501	8296
<i>R</i> <sup>a</sup>	0.0687	0.0562	0.0406
<i>R</i> <sub>w</sub> <sup>b</sup>	0.1981	0.1185	0.1063
	<b>4</b>	<b>5</b>	<b>6</b>
formula	C <sub>37</sub> H <sub>53</sub> O <sub>8</sub> PS	C <sub>31</sub> H <sub>41</sub> O <sub>8</sub> PS	C <sub>33</sub> H <sub>44</sub> F <sub>3</sub> O <sub>9</sub> PS
fw	688.82	604.67	704.71
crystal system	monoclinic	monoclinic	orthorhombic
space group	<i>P</i> 2 <sub>1</sub>	<i>P</i> 2 <sub>1</sub>	<i>P</i> 2 <sub>1</sub> 2 <sub>1</sub> 2 <sub>1</sub>
crystal size (mm)	1.00 × 0.45 × 0.30	0.60 × 0.05 × 0.03	0.75 × 0.40 × 0.05
<i>a</i> (Å)	17.1545(2)	13.701(2)	9.9547(2)
<i>b</i> (Å)	11.1392(1)	9.347(1)	17.7766(5)
<i>c</i> (Å)	19.8162(2)	15.544(2)	21.0860(6)
$\beta$ (deg)	91.4254(4)	112.281(4)	90.00
<i>V</i> (Å <sup>3</sup> )	3785.45(7)	1842.0(4)	3731.4(2)
<i>Z</i>	4	2	4
<i>D</i> <sub>calc</sub> (g/cm <sup>3</sup> )	1.209	1.090	1.254
$\mu_{\text{MoK}\alpha}$ (cm <sup>-1</sup> )	1.75	1.72	1.93
total reflns	13262	3345	6406
reflns with <i>I</i> > 2 $\sigma$ <i>I</i>	10784	2666	5541
<i>R</i> <sup>a</sup>	0.0525	0.1443	0.0459
<i>R</i> <sub>w</sub> <sup>b</sup>	0.1319	0.2897	0.0977
	<b>7</b>	<b>8</b>	<b>9</b>
formula	C <sub>33</sub> H <sub>44</sub> F <sub>3</sub> O <sub>11</sub> PS	C <sub>34</sub> H <sub>46</sub> F <sub>3</sub> O <sub>9</sub> P	C <sub>40</sub> H <sub>58</sub> F <sub>3</sub> O <sub>9</sub> P
fw	736.71	686.68	770.83
crystal system	monoclinic	monoclinic	orthorhombic
space group	<i>P</i> 2 <sub>1</sub>	<i>P</i> 2 <sub>1</sub>	<i>P</i> 2 <sub>1</sub> 2 <sub>1</sub> 2 <sub>1</sub>
crystal size (mm)	0.65 × 0.65 × 0.50	0.85 × 0.75 × 0.60	1.00 × 1.00 × 0.90
<i>a</i> (Å)	9.5531(1)	10.8623(2)	10.5287(2)
<i>b</i> (Å)	26.3363(4)	25.0460(4)	11.8268(2)
<i>c</i> (Å)	14.8612(2)	13.9799(3)	34.0252(7)
$\beta$ (deg)	105.0007(7)	109.2145(7)	90.00
<i>V</i> (Å <sup>3</sup> )	3611.56(8)	3591.5(1)	4236.8(1)
<i>Z</i>	4	4	4
<i>D</i> <sub>calc</sub> (g/cm <sup>3</sup> )	1.355	1.270	1.208
$\mu_{\text{MoK}\alpha}$ (cm <sup>-1</sup> )	2.06	1.42	1.28
total reflns	11517	12328	7239
reflns with <i>I</i> > 2 $\sigma$ <i>I</i>	10450	10496	6323
<i>R</i> <sup>a</sup>	0.0472	0.0527	0.0533
<i>R</i> <sub>w</sub> <sup>b</sup>	0.1255	0.1282	0.1369

$$^a R = \sum ||F_o| - |F_c|| / \sum |F_o|. \quad ^b R_w(F_o^2) = \{\sum w(F_o^2 - F_c^2)^2 / \sum wF_o^4\}^{1/2}.$$

the absence of meaningful connectivities precluded locating any solvent molecules (the calculated electron density for all the carbon atoms were higher than 3 e/Å<sup>3</sup>). The anisotropic refinements for **5** were restrained using the ISOR and SIMU instructions of the SHELX program for all atoms except those of phosphorus and sulfur atoms.

## Results and Discussion

Crystallographic data are summarized in Table 1. The atom-labeling schemes for **1–9** are given in the ORTEP plots of Figures 1–9, respectively. These figures were made using

ORTEP-III for Windows.<sup>15</sup> The hydrogen atoms are omitted for clarity. The thermal ellipsoids are shown at the 50% probability level. Selected bond parameters are given in Tables 2–10.

**Syntheses.** The polycyclic phosphoranes were quite difficult to synthesize because of competing reactions as outlined below. Due to the challenges, various approaches were analyzed. The simple method of reacting the polycyclic phosphite **13** with a diphenol proved to be too slow (Scheme

(15) Farrugia, L. J. *J. Appl. Crystallogr.* **1997**, *30*, 565.

**Table 2.** Selected Bond Lengths (Å) and Angles (deg) for **1**

P–O(4)	1.603(4)	P–O(5)	1.649(4)
P–O(6)	1.631(4)	P–O(7)	1.629(4)
P–O(8)	1.684(4)	P–O(9)	2.660(4)
S–O(9)	1.438(4)	S–O(10)	1.440(4)
O(4)–P–O(5)	97.6(2)	O(4)–P–O(6)	105.3(2)
O(4)–P–O(7)	101.8(2)	O(4)–P–O(8)	95.8(2)
O(4)–P–O(9)	177.2(2)	O(5)–P–O(6)	91.5(2)
O(5)–P–O(7)	85.2(2)	O(5)–P–O(8)	166.2(2)
O(5)–P–O(9)	80.6(2)	O(6)–P–O(7)	152.9(2)
O(6)–P–O(8)	88.5(2)	O(6)–P–O(9)	77.0(2)
O(7)–P–O(8)	88.5(2)	O(7)–P–O(9)	75.9(2)
O(8)–P–O(9)	85.9(2)	O(9)–S–O(10)	117.2(3)
C(15)–S–C(14)	104.6(3)	C(3)–O(4)–P	118.0(3)
C(5)–O(5)–P	107.6(3)	C(6)–O(6)–P	114.3(3)
C(9)–O(7)–P	132.6(4)	C(20)–O(8)–P	131.7(3)
S–O(9)–P	103.5(2)		

**Table 3.** Selected Bond Lengths (Å) and Angles (deg) for **2**

P–O(4)	1.598(2)	P–O(5)	1.646(3)
P–O(6)	1.626(3)	P–O(7)	1.676(2)
P–O(8)	1.641(2)	P–O(9)	2.618(2)
S–O(9)	1.440(3)	S–O(10)	1.431(3)
O(4)–P–O(5)	98.2(1)	O(4)–P–O(6)	104.3(1)
O(4)–P–O(7)	97.4(1)	O(4)–P–O(8)	100.4(1)
O(4)–P–O(9)	174.6(1)	O(5)–P–O(6)	91.6(1)
O(5)–P–O(7)	164.0(1)	O(5)–P–O(8)	85.6(1)
O(5)–P–O(9)	77.1(1)	O(6)–P–O(7)	87.9(1)
O(6)–P–O(8)	155.2(1)	O(6)–P–O(9)	78.8(1)
O(7)–P–O(8)	88.1(1)	O(7)–P–O(9)	87.1(1)
O(8)–P–O(9)	76.6(1)	O(10)–S–O(9)	118.1(2)
C(15)–S–C(16)	106.9(2)	S–O(9)–P	103.5(1)

**Table 4.** Selected Bond Lengths (Å) and Angles (deg) for **3**

P–O(4)	1.600(2)	P–O(5)	1.650(2)
P–O(6)	1.626(2)	P–O(7)	1.682(2)
P–O(8)	1.634(2)	P–O(9)	2.726(2)
S–O(10)	1.434(2)	S–O(9)	1.440(2)
O(4)–P–O(5)	97.94(9)	O(4)–P–O(6)	105.30(9)
O(4)–P–O(7)	95.80(8)	O(4)–P–O(8)	103.47(9)
O(4)–P–O(9)	176.22(7)	O(5)–P–O(6)	91.58(8)
O(5)–P–O(7)	165.88(9)	O(5)–P–O(8)	84.34(8)
O(5)–P–O(9)	79.44(7)	O(6)–P–O(7)	87.92(8)
O(6)–P–O(8)	151.23(9)	O(6)–P–O(9)	77.58(7)
O(7)–P–O(8)	89.33(8)	O(7)–P–O(9)	86.68(7)
O(8)–P–O(9)	73.67(7)	O(10)–S–O(9)	117.2(1)
C(15)–S–C(16)	103.4(1)	S–O(9)–P	100.60(9)

1). This resulted in an enone<sup>17</sup> and phosphates as major products; the expected phosphorane was a very minor product and difficult to separate. However, in one case, phosphorane **4** was successfully isolated in low yield. In the next effort, the plan to attach the glucofuranose moiety at the phosphite stage provided only the polycyclic phosphite and diphenol (Scheme 2), the same as the starting point shown in Scheme 1.

The third approach involved formation of a chlorophosphorane and treating this highly reactive phosphorane with the glucofuranose derivatives (two paths are shown in Scheme 3). This approach was found to be fast and provided better yields of the expected phosphoranes. Phosphoranes **1–3** were synthesized using this approach. Their crystallized

(16) Chandrasekaran, A.; Day, R. O.; Holmes, R. R. *J. Am. Chem. Soc.* **1997**, *119*, 11434–11441.

(17) Izuoka, A.; Miya, S.; Sugawara, T. *Tetrahedron Lett.* **1988**, *29*, 5673–5676. Dean, F. M.; Herbin, G. A.; Matkin, D. A.; Price, A. W.; Robinson, M. L. *J. Chem. Soc., Perkin Trans. 1* **1980**, 1986–1993. Aleksniuk, O.; Cohen, S.; Bialy, S. E. *J. Am. Chem. Soc.* **1995**, *117*, 9645–9652.

**Table 5.** Selected Bond Lengths (Å) and Angles (deg) for **4**

P(1)–O(4)	1.618(2)	P(2)–O(4A)	1.613(2)
P(1)–O(5)	1.652(3)	P(2)–O(5A)	1.659(3)
P(1)–O(6)	1.655(3)	P(2)–O(6A)	1.658(3)
P(1)–O(7)	1.666(3)	P(2)–O(7A)	1.654(3)
P(1)–O(8)	1.665(3)	P(2)–O(8A)	1.674(2)
P(1)–S(1)	2.599(1)	P(2)–S(2)	2.666(1)
O(4)–P(1)–O(5)	97.8(1)	O(4A)–P(2)–O(5A)	98.7(1)
O(4)–P(1)–O(6)	100.7(1)	O(4A)–P(2)–O(6A)	100.8(1)
O(4)–P(1)–O(7)	91.5(1)	O(4A)–P(2)–O(7A)	92.5(1)
O(4)–P(1)–O(8)	92.9(1)	O(4A)–P(2)–O(8A)	94.0(1)
O(5)–P(1)–O(6)	91.3(1)	O(5A)–P(2)–O(6A)	90.8(1)
O(5)–P(1)–O(7)	87.3(2)	O(5A)–P(2)–O(7A)	87.5(2)
O(5)–P(1)–O(8)	169.0(1)	O(5A)–P(2)–O(8A)	167.3(1)
O(6)–P(1)–O(7)	167.8(1)	O(6A)–P(2)–O(7A)	166.7(1)
O(6)–P(1)–O(8)	89.2(1)	O(6A)–P(2)–O(8A)	88.2(1)
O(8)–P(1)–O(7)	89.9(2)	O(7A)–P(2)–O(8A)	90.6(1)
O(4)–P(1)–S(1)	172.13(9)	O(4A)–P(2)–S(2)	171.27(9)
O(5)–P(1)–S(1)	88.4(1)	O(5A)–P(2)–S(2)	88.2(1)
O(6)–P(1)–S(1)	83.99(9)	O(6A)–P(2)–S(2)	84.40(9)
O(7)–P(1)–S(1)	83.85(9)	O(7A)–P(2)–S(2)	82.3(1)
O(8)–P(1)–S(1)	80.78(9)	O(8A)–P(2)–S(2)	79.10(8)
C(15)–S(1)–C(16)	101.3(2)	C(15A)–S(2)–C(16A)	101.1(2)
C(15)–S(1)–P(1)	88.7(1)	C(16)–S(1)–P(1)	89.2(1)

**Table 6.** Selected Bond Lengths (Å) and Angles (deg) for **5**

P–O(4)	1.63(1)	P–O(5)	1.61(1)
P–O(6)	1.68(1)	P–O(7)	1.63(1)
P–O(8)	1.72(1)	P–S	2.695(8)
O(4)–P–O(5)	98.4(6)	O(4)–P–O(6)	01.1(6)
O(4)–P–O(7)	92.8(6)	O(4)–P–O(8)	96.2(6)
O(5)–P–O(6)	91.2(6)	O(5)–P–O(7)	87.5(7)
O(5)–P–O(8)	165.2(7)	O(6)–P–O(7)	166.1(6)
O(6)–P–O(8)	87.9(6)	O(7)–P–O(8)	89.8(6)
O(4)–P–S	172.8(5)	O(5)–P–S	86.8(4)
O(6)–P–S	83.7(4)	O(7)–P–S	82.4(4)
O(8)–P–S	78.4(5)	C(16)–S–C(15)	102.8(8)
C(16)–S–P	86.9(7)	C(15)–S–P	88.2(7)

**Table 7.** Selected Bond Lengths (Å) and Angles (deg) for **6**

P–O(5)	1.656(2)	P–O(6)	1.643(2)
P–O(7)	1.682(2)	P–O(8)	1.695(2)
P–O(9)	1.621(2)	P–S	2.542(1)
O(5)–P–O(6)	91.9(1)	O(5)–P–O(7)	87.6(1)
O(5)–P–O(8)	171.0(1)	O(5)–P–O(9)	96.0(1)
O(6)–P–O(7)	168.6(1)	O(6)–P–O(8)	89.2(1)
O(6)–P–O(9)	98.1(1)	O(7)–P–O(8)	89.5(1)
O(7)–P–O(9)	93.2(1)	O(8)–P–O(9)	92.6(1)
O(5)–P–S	87.37(8)	O(6)–P–S	84.41(8)
O(7)–P–S	84.23(7)	O(8)–P–S	83.85(7)
O(9)–P–S	175.65(8)	C(15)–S–C(16)	107.3(1)
C(15)–S–P	90.3(1)	C(16)–S–P	89.7(1)

yield is much lower than the actual yield of the crude products because of partial solubility in ethanol, which was found to be the best solvent for their crystallization (the phosphorus NMR data suggested yields in the range of 50–60% in the reaction mixture). This approach worked well only when there was a donor atom present in the diphenol. Surprisingly, even this method did not work for the methylene-bridged diphenols, which were to be used for comparison in measuring donor interaction. Only phosphates and enones were obtained.

Hence, a fourth approach was attempted in which trifluoroethoxy–hydroxy phosphoranes **6–9** were synthesized with the idea that heating them would produce the expected polycyclic phosphoranes, especially the inaccessible phosphoranes with the methylene-bridged diphenol moiety that are analogues of the sulfur-bridged systems **4** and **5**. Though this approach seemed to work reasonably well based on the

**Table 8.** Selected Bond Lengths (Å) and Angles (deg) for **7**

P(1)–O(5)	1.663(2)	P(2)–O(5A)	1.666(2)
P(1)–O(6)	1.604(2)	P(2)–O(6A)	1.604(2)
P(1)–O(7)	1.618(2)	P(2)–O(7A)	1.615(2)
P(1)–O(8)	1.617(2)	P(2)–O(8A)	1.617(2)
P(1)–O(9)	1.643(3)	P(2)–O(9A)	1.638(2)
S(1)–O(11)	1.428(3)	S(2)–O(10A)	1.433(3)
S(1)–O(10)	1.428(3)	S(2)–O(11A)	1.449(3)
O(5)–P(1)–O(6)	90.7(1)	O(5A)–P(2)–O(6A)	90.5(1)
O(5)–P(1)–O(7)	90.4(1)	O(5A)–P(2)–O(7A)	94.7(1)
O(5)–P(1)–O(8)	94.7(1)	O(5A)–P(2)–O(8A)	90.3(1)
O(5)–P(1)–O(9)	174.6(1)	O(5A)–P(2)–O(9A)	174.4(1)
O(6)–P(1)–O(7)	120.2(1)	O(6A)–P(2)–O(7A)	119.4(1)
O(6)–P(1)–O(8)	126.2(1)	O(6A)–P(2)–O(8A)	128.2(1)
O(6)–P(1)–O(9)	85.0(1)	O(6A)–P(2)–O(9A)	85.1(1)
O(7)–P(1)–O(8)	113.3(1)	O(7A)–P(2)–O(8A)	112.2(1)
O(7)–P(1)–O(9)	90.2(1)	O(7A)–P(2)–O(9A)	90.5(1)
O(8)–P(1)–O(9)	89.6(1)	O(8A)–P(2)–O(9A)	89.6(1)
O(11)–S(1)–O(10)	118.9(2)	O(10A)–S(2)–O(11A)	118.7(2)
C(15)–S(1)–C(16)	109.6(2)	C(16A)–S(2)–C(15A)	110.0(1)

**Table 9.** Selected Bond Lengths (Å) and Angles (deg) for **8**

P(1)–O(5)	1.664(2)	P(2)–O(15)	1.665(2)
P(1)–O(6)	1.599(2)	P(2)–O(16)	1.597(2)
P(1)–O(7)	1.607(2)	P(2)–O(17)	1.610(2)
P(1)–O(8)	1.614(2)	P(2)–O(18)	1.612(2)
P(1)–O(9)	1.654(2)	P(2)–O(19)	1.655(2)
O(5)–P(1)–O(6)	90.7(1)	O(15)–P(2)–O(16)	90.7(1)
O(5)–P(1)–O(7)	94.6(1)	O(15)–P(2)–O(17)	96.0(1)
O(5)–P(1)–O(8)	91.2(1)	O(15)–P(2)–O(18)	90.5(1)
O(5)–P(1)–O(9)	174.8(1)	O(15)–P(2)–O(19)	173.1(1)
O(6)–P(1)–O(7)	121.3(1)	O(16)–P(2)–O(17)	117.5(1)
O(6)–P(1)–O(8)	125.3(1)	O(16)–P(2)–O(18)	129.0(1)
O(6)–P(1)–O(9)	84.6(1)	O(16)–P(2)–O(19)	84.2(1)
O(7)–P(1)–O(8)	113.0(1)	O(17)–P(2)–O(18)	113.0(1)
O(7)–P(1)–O(9)	89.7(1)	O(17)–P(2)–O(19)	90.5(1)
O(8)–P(1)–O(9)	89.8(1)	O(18)–P(2)–O(19)	89.1(1)

**Table 10.** Selected Bond Lengths (Å) and Angles (deg) for **9**

P–O(5)	1.661(2)	P–O(6)	1.603(2)
P–O(7)	1.621(2)	P–O(8)	1.615(2)
P–O(9)	1.646(2)		
O(5)–P–O(6)	90.5(1)	O(5)–P–O(7)	93.6(1)
O(5)–P–O(8)	91.1(1)	O(5)–P–O(9)	175.1(1)
O(6)–P–O(7)	119.2(1)	O(6)–P–O(8)	124.9(1)
O(6)–P–O(9)	85.2(1)	O(7)–P–O(8)	115.6(1)
O(7)–P–O(9)	90.5(1)	O(8)–P–O(9)	89.5(1)

absence of OH and OCH<sub>2</sub>CF<sub>3</sub> protons and the disappearance of aromatic ring shielding effects, without a notable <sup>31</sup>P NMR shift change in the sample used for melting point determinations, it was difficult to reproduce on a decent reaction scale. There was no reaction when phosphorane **9** was refluxed in toluene for 24 h, whereas heating **9** to about 180 °C for 4 min resulted in complete thermal decomposition to yield phosphates. The structures of the phosphoranes **6–9** were studied in order to compare with our previously reported fluorophosphoranes.<sup>3</sup> Phosphoranes **6–9** are the first biologically relevant bicyclic pentaoxyphosphoranes.

Reactions of the trifluoroethoxy phosphites with isopropylidene-xylofuranose, thymidine, adenosine, and inosine showed the formation of interesting phosphoranes having a variety of isomers based on the <sup>31</sup>P NMR data, in addition to some phosphates. However, the phosphorane mixtures were either completely soluble in various solvents ranging from hexane to ethanol or provided only amorphous solids. This precluded the purification and separation of any phosphorane from this interesting system. Further studies are needed in this direction.

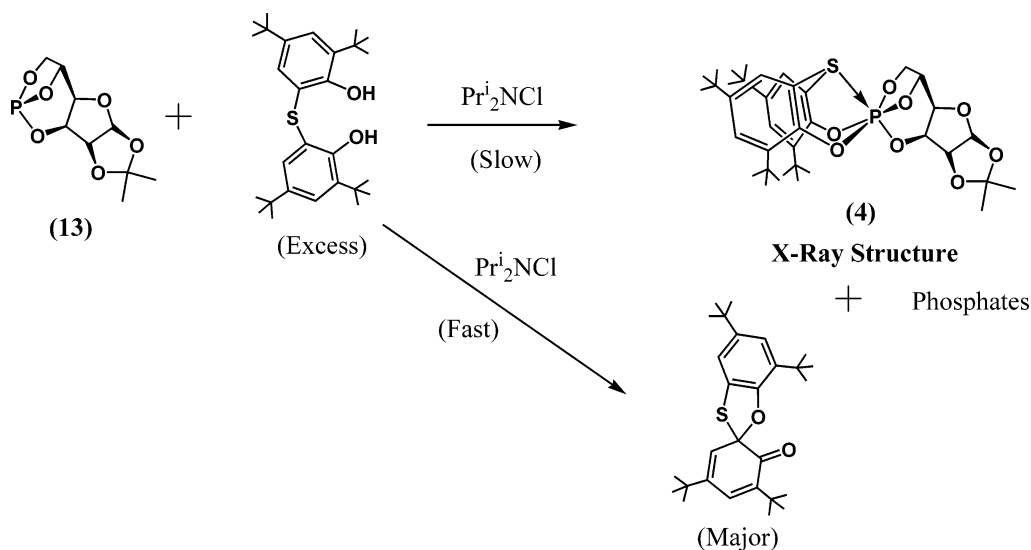
**Structure of Polycyclic Phosphoranes 1–5.** The polycyclic pentaoxyphosphoranes **1–5** (Chart 2, Figures 1–5) have a very narrow range of the phosphorus–donor distance (2.73–2.60 Å) irrespective of the donor atom (S or O). This suggests a possible ring constraint or the weak electron-withdrawing effect of the three alkoxy groups or both. Efforts to obtain a non-donor CH<sub>2</sub> group containing polycyclic phosphorane were not successful, and hence, at present, the cause for this narrow range remains ambiguous. In monocyclic phosphoranes with the SO<sub>2</sub> donor group, there was a dynamic equilibrium between penta- and hexacoordinated phosphoranes.<sup>1b,11,16</sup> However, in this polycyclic system, the equilibrium has been replaced with a stable structure in the hexacoordinated form. It is most likely due to the inability to reach the more stable trigonal bipyramidal (TBP) geometry of the pentacoordinated form caused by the ring constraints, which would force it to a square pyramidal (SP) geometry where the donor atom would be closer to the phosphorus atom.

**Mechanism of Hexacoordination.** Generally, it is considered that pentacoordination to hexacoordination occurs through a square pyramidal geometry (SP) from a trigonal bipyramidal geometry (TBP).<sup>18</sup> Recently, we have understood that in the sulfonyl donor system (SO<sub>2</sub>) there is another intermediate stage in this change where the TBP-ee ring (with an eight-membered ring in a diequatorial position) undergoes a change to the TBP-ae ring (leaving the eight-membered ring occupying axial–equatorial sites).<sup>1b</sup> The SP distortion is only partial, and this allows one to easily see which were axial and equatorial groups in the original TBP-ae intermediate. This results in nonequivalence for the two parts of the eight-membered ring-forming diphenol moiety (Scheme 4), which can be seen from the P–O distances, the O–P–O angles, and also the nonequivalence in the proton NMR data (see below). Thus, the structural changes for this series of phosphoranes with donor-containing eight-membered rings follow the mechanistic sequence (irrespective of the donor atom) TBP(ee) → TBP(ae) → [TBP(ae)–SP] → octahedral.

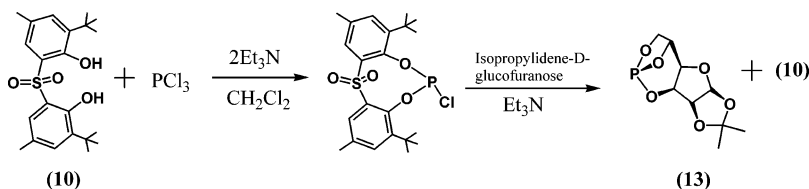
In the hexacoordinated phosphoranes with the sulfonyl groups (**1–3**), the axial–equatorial difference between the diphenoxy eight-membered ring oxygens can be seen. This is seen from the longer P–O bond distances for the O8 oxygen in **1** and the O7 oxygens in **2** and **3**, which represent the O<sup>1</sup> shown in Scheme 4. The remaining oxygen of the eight-membered ring (O<sup>2</sup> type) shows a shorter distance. The ranges for these two types of oxygens are 1.676–1.684 for the O<sup>1</sup> type and 1.629–1.641 for the O<sup>2</sup> type. Similarly, the trans O–P–O angles for these O<sup>1</sup> type oxygens (164.0–166.2°) are closer to 180°, and the angles for O<sup>2</sup> type oxygens (151.2–155.2°) are farther from 180°. This suggests that some of the TBP-ae intermediate characters are still present. In the case of stronger sulfur donor systems (in **4–6**), the bond parameter differences are minor and the structure is displaced between a square pyramid and an octahedron without any TBP distortions.

(18) Deiters, J. A.; Holmes, R. R. *Phosphorus, Sulfur Silicon Relat. Elem.* **1998**, *123*, 329–340.

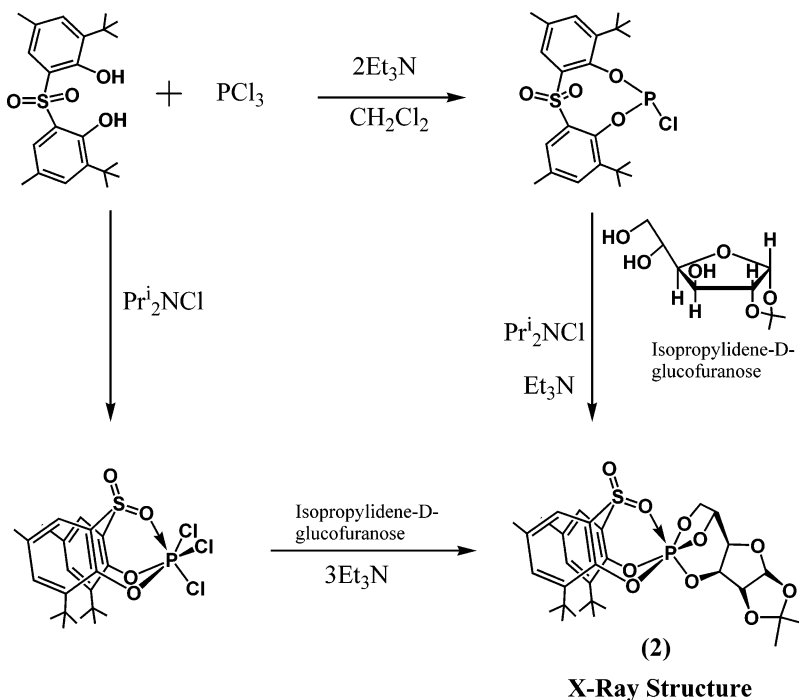
Scheme 1



Scheme 2



Scheme 3



The differences observed in **1–3**, as discussed above, also result in the two *tert*-butyl protons and aryl-CH protons showing nonequivalence in the proton NMR spectra. The *tert*-butyl, aryl-CH<sub>3</sub>, and aryl-H protons show a difference (range for aryl-H) of 0.12, 0.11, and 0.37 ppm in **1** and 0.16, 0.11, and 0.39 ppm in **2**. In the similar sulfur donor system in **5**, the differences are only 0.02, 0.01, and 0.19 ppm, respectively. In the slightly different phosphorane **4** with the

sulfur donor interaction, the difference for similar *tert*-butyl groups is 0.01 ppm and a 0.11 ppm range for aryl-H. This clearly shows the huge nonequivalence in the eight-membered ring in the case of the sulfonyl donor system. The minor differences seen in the sulfur donor system are due to the spatial inequivalence of the chiral glucose moiety. The larger difference in the sulfonyl system is due to the sum of the spatial difference caused by the glucose moiety and, in



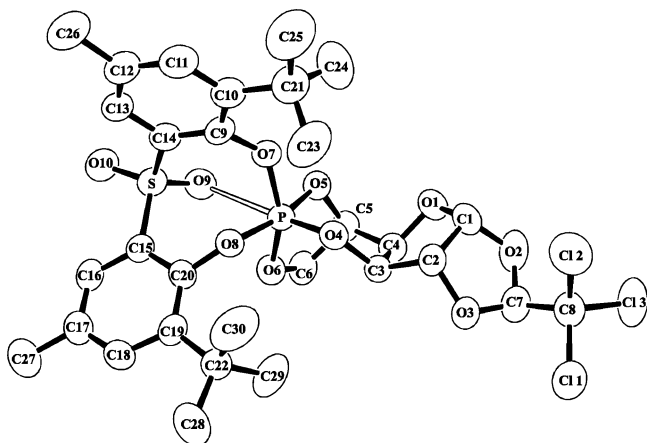


**Figure 1.** ORTEP diagram of **1** (dichloromethane solvent molecule is not shown).

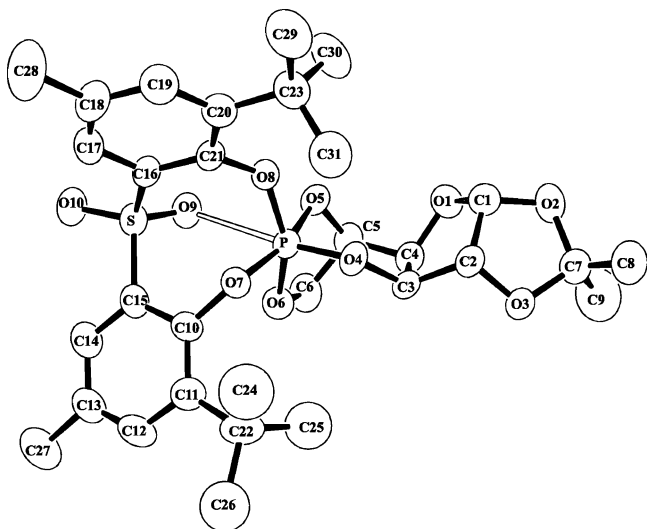


**Figure 2.** ORTEP diagram of **2**. The methyl carbons attached to C23 were disordered, and only one set is shown.

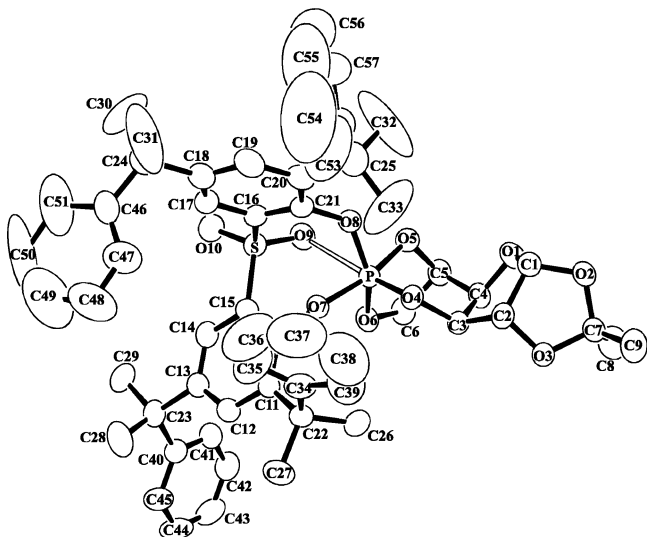


**Figure 3.** ORTEP diagram of **3**. The atoms C11 (behind C36) and C52 (behind C53) are not labeled.

most part, by the electronic factors of the remaining TBP distortion. However, it is still not clear whether the continued presence of TBP distortion in the hexacoordinated state of

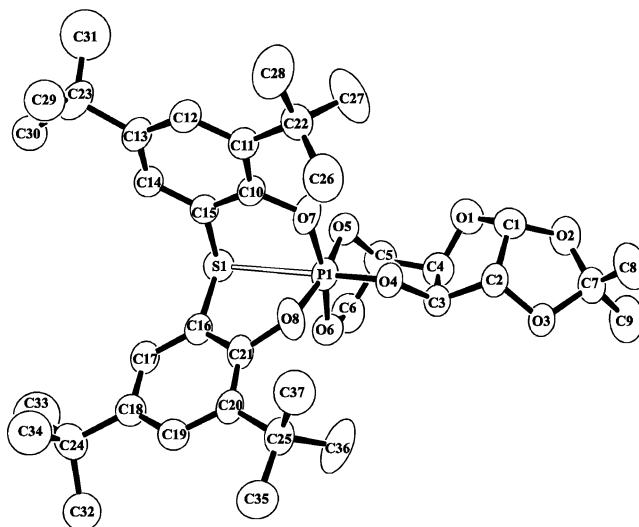


**Figure 4.** ORTEP diagram of **4**. Only one of the two independent molecules is shown. The methyl carbons attached to C23 and C24 were disordered, and only one set is shown.

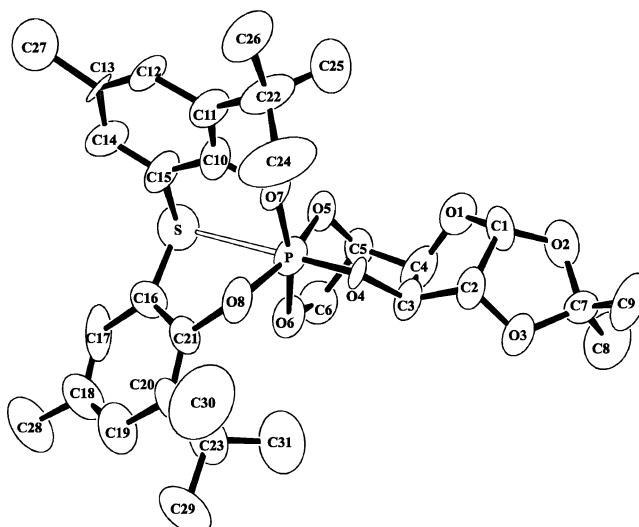
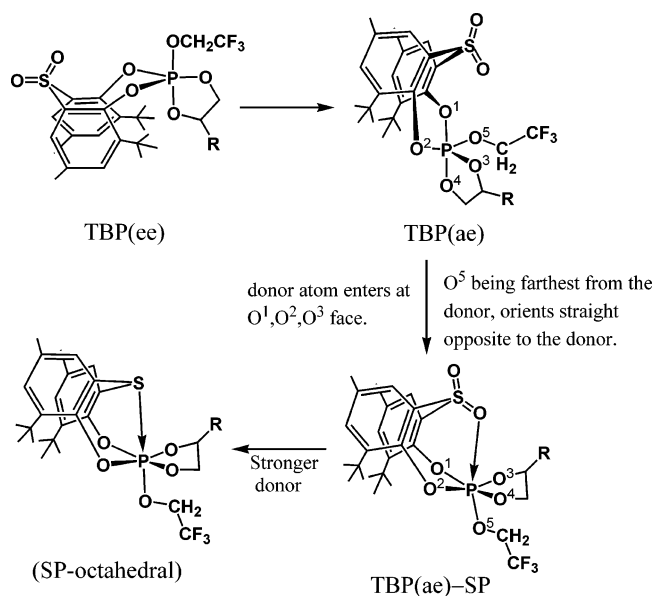


**Figure 5.** ORTEP diagram of **5**.

sulfonyl-containing phosphoranes is due to the weaker donor nature or due to their larger donor ring size. It should be noted that the sulfur donor results in a five-membered donor ring, whereas the sulfonyl oxygen leads to a six-membered donor ring.

**Structure of Bicyclic Pentaoxyphosphoranes 6–9.** In the bicyclic phosphoranes **6–9** (Chart 2 and Figures 6–9), one free hydroxyl group is present in the glucofuranose moiety and one trifluoroethoxy group resides on phosphorus. Phosphorane **6** shows a hexacoordinated phosphorus atom with the eight-membered ring having a syn conformation. All the other pentaoxyphosphoranes **7–9** have a penta-coordinated phosphorus atom with a TBP geometry where the eight-membered ring occupies two equatorial positions and the five-membered ring occupies axial–equatorial positions, as expected. The eight-membered rings also possess an anti conformation. In phosphorane **7**, which has a weak  $\text{SO}_2$  donor group, an equilibrium exists between penta- and hexacoordinated phosphoranes in solution, where the penta-coordinated isomer is the major isomer. In the crystalline

Scheme 4



state, the pentacoordinated form also prevails. This is in agreement with our earlier observation of monocyclic phosphoranes that possessed three alkoxy groups.<sup>11,16</sup> However, a recent bulkier diphenoxy system showed an increased preference for the hexacoordinated form (Scheme 5).<sup>1b</sup>

In our earlier study of fluorotetraoxy bicyclic phosphoranes (18–19), we observed that the bulky secondary alkoxy group never occupied the very crowded endo-axial position (Scheme 6). Although, both in the monocyclic phosphoranes 20–21 and in the bicyclic systems 18–19 (Scheme 6), the secondary alkoxy group often occupied the axial positions,<sup>3</sup> in the present pentaoxy bicyclic systems (in 7–9), the bulky secondary alkoxy group always occupies the most crowded endo-axial position, even though it is the energetically least favored form<sup>3b</sup> (see the NMR discussion below).

**Isomerism.** Earlier, we have observed hexa- and penta-coordinated phosphoranes remaining in equilibrium in solution when the sulfonyl group is present as part of the eight-membered ring system and there are poor electron-withdrawing substituents on phosphorus, such as alkoxy<sup>1b,11,16</sup> or phenyl<sup>16</sup> groups. A similar equilibrium is observed in the

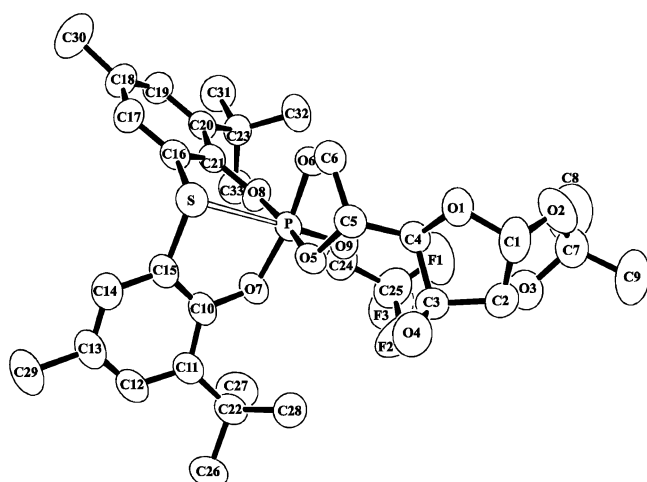


Figure 6. ORTEP diagram of 6.

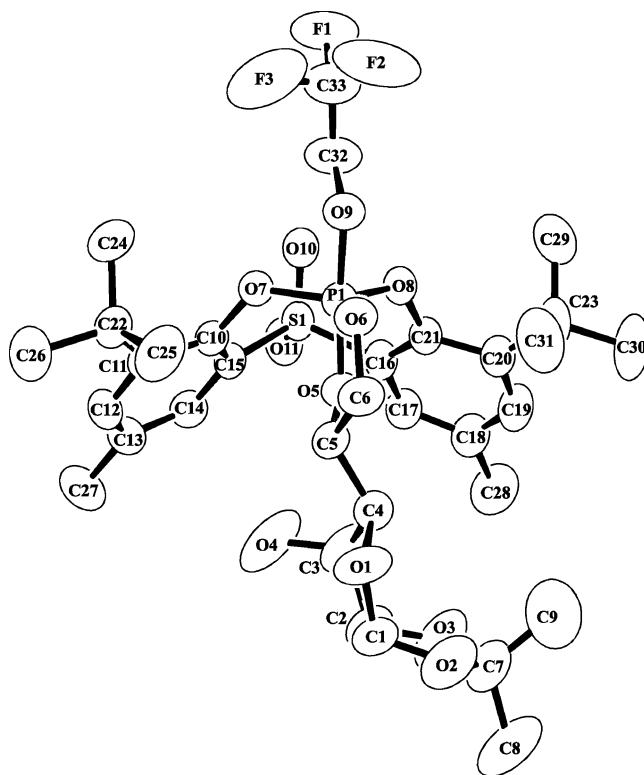


Figure 7. ORTEP diagram of 7.

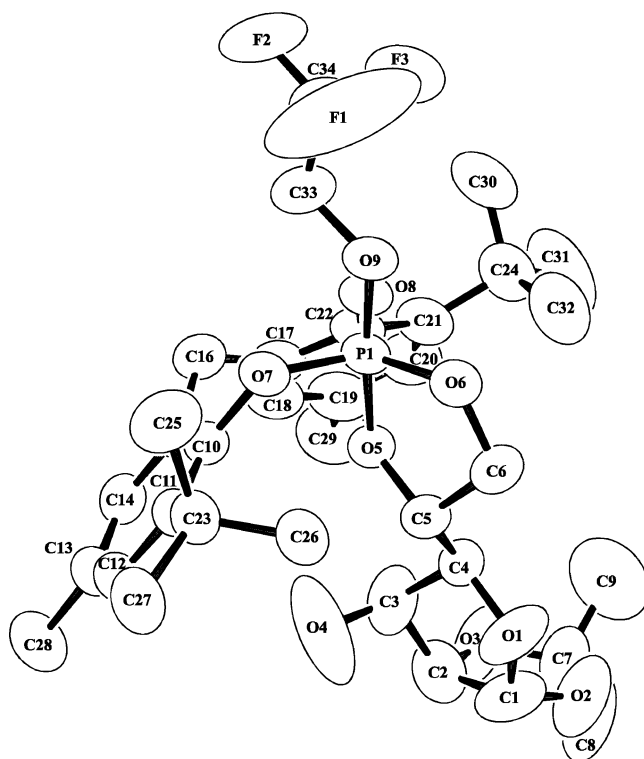
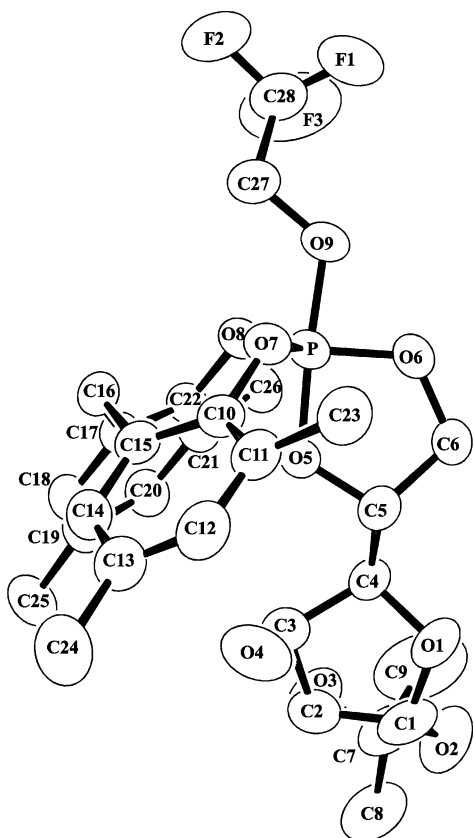


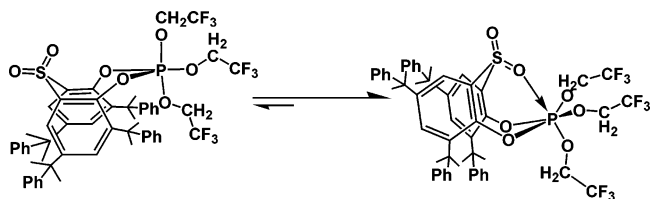
Figure 8. ORTEP diagram of 8. Only one of the two independent molecules is shown. The atom C15 is hidden behind C25.

case of the bicyclic phosphorane 7, with the pentacoordinated form being the dominant isomer, which remains as the only isomer in the solid state, as referred to above in the section on the structures of bicyclic pentaoxyphosphoranes 7–9. However, in the case of polycyclic phosphoranes 1–3, there is no such isomerism. Only one isomer, the hexacoordinated



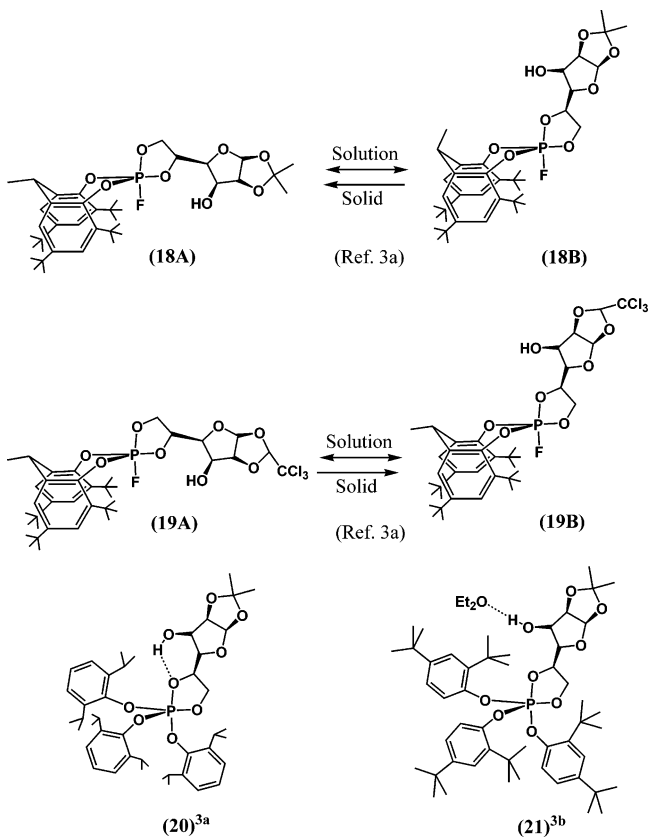
**Figure 9.** ORTEP diagram of **9**. The methyl carbons of the *tert*-butyl groups, attached to C23–C26, have been omitted for clarity.

#### Scheme 5

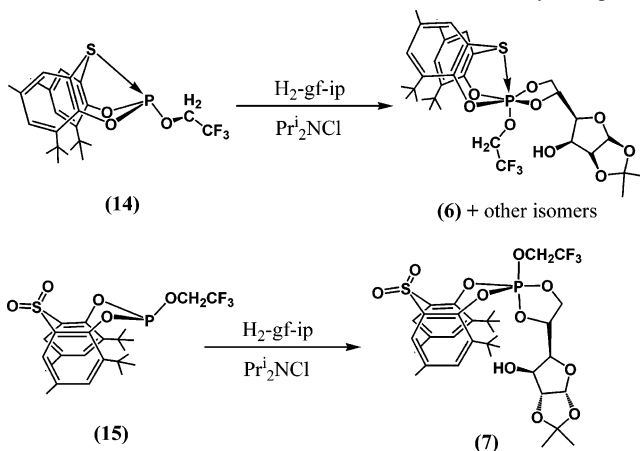


form, is observed in both solution and solid states. When there were no donor atoms, we still observed isomerism resulting from the different orientations possible for the carbohydrate-based five-membered ring.<sup>3b</sup> As seen from Scheme 6, the primary and secondary alkoxy groups of the carbohydrate moiety can occupy any of the three possible positions, equatorial, *exo*-axial, or *endo*-axial. However, in the bicyclic phosphoranes without a donor interaction (**7**–**9**), no such isomerism was observed. In all these three phosphoranes, the secondary alkoxy group occupied the *endo*-axial position in both solution and solid states. Generally, little isomerism has been observed when there is a sulfur donor atom in the eight-membered ring. However, in the reaction mixture of phosphorane **6**, nearly 20 isomers were observed in solution, though only two were structurally characterized. From the <sup>31</sup>P NMR data, there were three distinct sets suggesting three basic structures (–48 to –53, –73 to –77, and –85 to –89 ppm). One set, in the region –48 to –53 ppm, is expected to possess a five-membered ring formed by the glucose moiety, whereas the other two sets are expected to have a six-membered ring involving the glucose moiety.

#### Scheme 6



#### Scheme 7 Conformational Retention of the Trifluoroethoxy Group



To summarize our discussion on isomerism, we offer the following explanation. The trifluoroethoxy group maintains its orientation similar to that found in the starting phosphite. So, it seems that there is a retention of the phosphorus geometry when it goes from phosphite to phosphorane (which was not known before). In the case of the fluorine system that we reported earlier,<sup>3</sup> the fluorine is too small to stop fluxionality. As a result, the starting phosphite and its phosphorane products have a dynamic equilibrium between two isomers.

Scheme 7 shows the conformational retention for the trifluoroethoxy group in a similar position. Possibly the steric effect between one of the *tert*-butyl groups and the furanose ring (with further bulk added by the hydroxyl group and isopropylidene ring) prevents the secondary alkoxy group

from occupying the equatorial position. Then the molecular rigidity forces it to occupy the *exo*-axial position. In this orientation, the furanose ring is farther away from the *tert*-butyl group. Using Figure 7 as a guide, if the secondary alkoxy group occupied the equatorial position, we would have to place the furanose between C6 and C25 where there is hardly enough space (to retain the chirality, the group has to be placed opposite to the current side). However, when the five-membered ring is in the *endo* side, as seen in **18A** and **19A** (Scheme 6), the furanose group is sufficiently away from the *tert*-butyl group. In short, when the bulky substituents are farther from the central atom, the best orientation for that group is the axial position. This explains all the conformations we have observed so far, even though many were unexpected before the actual observations.

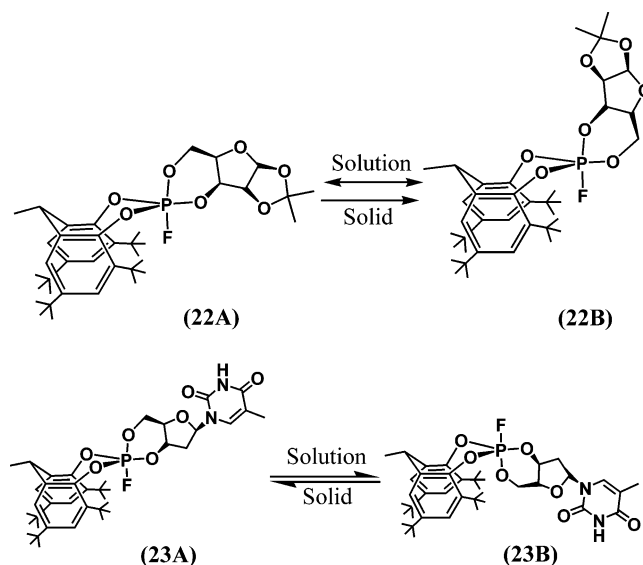
**NMR Studies.** The solution NMR data are in agreement with the assigned solid state structures. Generally, the phosphorus NMR data is not able to distinguish between the penta- and hexacoordination at phosphorus. However, it was quite easy to detect the presence of the five-membered rings that caused a deshielding at the phosphorus atom and gave chemical shifts that appeared in the downfield region (between  $-60$  and  $-50$  ppm for all phosphoranones, **1–9**), compared with the normally expected  $-80$  ppm range for larger rings. In the proton NMR spectra of pentacoordinated phosphoranones **7–9**, very high shieldings were observed, which we attributed to the influence of the aromatic rings. This feature is known for the groups that are present in the *endo*-axial position.<sup>3a</sup> This made it easy to identify the position of the secondary alkoxy group.

The hydroxy protons of **7** and **8** appeared in the negative chemical shift region, and in **9** the OH proton resonated at 1.55 ppm. Additionally, the secondary alkyl-OCH protons of **7–9** appeared at 2.45–2.51 ppm; other OCH protons resonated in the range 3.1–4.3 ppm. Thus, the proton NMR data clearly showed that in solution the bulkier secondary alkoxy groups occupied the sterically crowded *endo*-axial position, in contrast to that observed in the fluorophosphoranones.<sup>3</sup> In addition, the proton NMR data showed nonequivalence for the diphenol moiety that arises due to the pseudoaxial-equatorial orientation of the eight-membered ring (a description is given in the Mechanism of Hexacoordination section earlier, which is based more on electronic effects). In pentacoordinated phosphoranones, there is a partial and smaller nonequivalence that arises due to the asymmetric nature of the five-membered ring (based more on spatial effects).

**Stability of Phosphoranones.** Phosphoranones **1–9** are very stable to moisture. In fact, the polycyclic phosphoranones **1–4** were so stable that they were recrystallized in atmospheric conditions in commercial alcohol containing traces of water. During the recrystallization process that lasted over several weeks or months, only a small amount of decomposition was observed. The extremely high stability provides an insight into the pathways through which a possible hydrolysis/alcoholysis might occur. Such nucleophilic reactions can occur by a P–O bond cleavage through either a dissociative or an associative pathway. If dissociation is the preferred

pathway of hydrolysis, the introduction of bulky groups or strained small rings or cages would be a destabilizing influence and promote hydrolysis. However, if the associative pathway is the preferred route, then the introduction of bulky groups and a number of rings would act as a stabilizing influence and reduce or stop hydrolysis. Were the dissociative pathway in operation, we would have seen only the hydrolyzed products for phosphoranones **1–4** when kept in moist alcohols for weeks. The absence of such decay and the unexpectedly high stability provides an insight suggesting that the associative pathway is preferred for the hydrolysis/alcoholysis reactions of phosphoranones in this system.

**Biochemical Implications.** In the area of promiscuous phosphoryl-transfer enzymes, the present work provides a mechanism for such enzymes to conduct different reactions at the same active site. For example,<sup>19</sup> chymotrypsin catalyzes the hydrolysis of a number of different substrates initiated by attack of a serine residue at a carbon atom that is thought to lead to similar tetrahedral activated states. Chymotrypsin also catalyzes the reaction at a tetrahedral phosphoryl group, which leads to a proposed trigonal bipyramidal activated state.<sup>19</sup> Thus, the active site of chymotrypsin is able to catalyze both amidase and phosphotriesterase reactions. Our recent publications established the X-ray structure of several biorelevant phosphoranones (**18–21**), one xylofuranose-based phosphorane (**22**)<sup>3b</sup> and one thymidine-based phosphorane



(**23**).<sup>3a</sup> In solution, the bicyclic phosphoranones **18**, **19**, and **22** showed dynamic equilibrium between two isomeric forms. The phosphorane **23** showed a static conversion between two isomers, one in the solid state and the other in solution. The monocyclic phosphoranones **20** and **21** showed fluxionality similar to the nonbiorelevant phosphoranones studied previously.<sup>20</sup> Furthermore, the phosphoranones retain their structural

(19) O'Brien, P. J.; Herschlag, D. *Chem. Biol.* **1999**, *6*, R91–105.

(20) Holmes, R. R. *Pentacoordinated Phosphorus — Structure and Spectroscopy*, ACS Monograph 175; American Chemical Society: Washington, D. C., 1980; Vol. I, p 479. Holmes, R. R. *Pentacoordinated Phosphorus — Reaction Mechanisms*; ACS Monograph 176, American Chemical Society: Washington, DC, 1980; Vol. I, p 237.



integrity going from the solid-state structures to solution, as is the case in the present work. Also in the present work, phosphorane **6** exhibits 20 isomers in solution and two of them have been characterized by X-ray diffraction. In addition, the bicyclic phosphorane **7** exists in an equilibrium between penta- and hexacoordinated isomeric forms. The rapid exchange process between these two geometries reorients the nucleotidyl or carbohydrate component of the trigonal bipyramidal phosphorane. At an active site, this type of pseudorotational behavior provides a mechanism that could bring another active site residue into play and account for a means for phosphoryl-transfer enzymes to express promiscuous behavior. Pseudorotation, a well-founded process in nonenzymatic phosphorus chemistry,<sup>20</sup> may have an

application in the future of phosphoryl-transfer enzyme chemistry.

**Acknowledgment.** The research presented here was supported by the donors of the Petroleum Research Fund, administered by the American Chemical Society, and is gratefully acknowledged. We thank the X-ray Structural Characterization Laboratory at the chemistry department supported by the University of Massachusetts and the National Science Foundation (grant CHE-9974648).

**Supporting Information Available:** Cif data. This material is available free of charge via the Internet at <http://pubs.acs.org>.

IC061596F